Distinct spatiotemporal movement properties reveal sub-modalities in crawling cell types

Quantifying movement is a powerful window into cellular functions. However, cells can generate movement through a variety of complex mechanisms. Here, we generate a flexible framework for comparing an especially variable type of motility: cellular crawling.

Contributors (A-Z)

Prachee Avasthi, Feridun Mert Celebi, Megan L. Hochstrasser, Ryan York

Version 4 · Mar 31, 2025

Purpose

In this pub, we present a new framework for analyzing a form of organismal movement that is notably hard to study: cellular crawling. We show how the framework can be used to study various aspects of crawling and demonstrate its utility in comparing the movement of diverse cell types and species. We find that changes in cell shape over time can be mapped by a two-dimensional 'movement space' which can be used to identify differences in cell type and state across a number of aspects of time and space. These results will be of interest to biologists focusing on cell motility and its mechanistic bases. In addition, this resource will be of use to behavioral scientists

broadly defined, especially those working with organisms that display complex and unpredictable shapes during movement.

- This pub is part of the **platform effort**, "Genetics: Decoding evolutionary drivers across biology." Visit the narrative for more background and context.

- All associated **code** is available in this GitHub repository.

- A full **walkthrough of the code base** for the framework appears in a series of companion notebooks.

Background and goals

Movement is a central component of life. Key biological processes — bacterial quorum sensing [1], fungal zoospore phototaxis [2], predation by ciliates [3], animal behavior broadly defined — all depend on complex motility patterns that reflect diverse biological processes. Movement, construed in this way, can thus be used as an accessible handle for studying otherwise intractably complex biology. For example, in animals, behavior is a key window into the function of nervous systems [4]. Similarly, the ciliary movements of individual cells are a window into the complex dynamics of the actin cytoskeleton as this network is responsible for cell protrusion, adhesion, and contractility. Organismal movement is also a relatively accessible and cost-effective phenotype to measure, one that can be interrogated in diverse organisms that may lack genetic access or reliable reagents. For these reasons, generating tools that can quantitatively compare movement across broad swaths of organisms may provide one of the cheapest and highest-impact ways to map and dissect phenotypic diversity across the tree of life.

This work is part of a broader effort to map the evolution of movement types among unicellular eukaryotes. These species display a variety of ways to move that are associated with extreme morphological and physiological diversity. We are generating methods for mapping this diversity and associating it with genetic variation in order to broadly dissect the molecular bases of unicellular behavior. As an initial step, we explored how to map an especially troublesome type of motility: cellular crawling.

Cellular crawling is one of the main modes of locomotion employed by Eukaryotic cells. Crawling is generated when actin-driven protrusions adhere to a surface, allowing the cell's mass to be pulled along [5]. Crawling has historically been binned into two types (though we anticipate that quantitative analyses may highlight additional sub-modalities): a slower, mesenchymal form, favored by immune cells and keratocytes, and a faster, amoeboid form, employed by *Dictyostelium* slime molds and other quick-moving unicellular organisms [5]. The constant deformation of the cell's shape during crawling differentiates it from other modes of locomotion, such as cilia-based swimming, and a variety of sophisticated computational models have been proposed to describe the generation of crawling from internal cellular dynamics [6][7][8][9][10][11][12][13]. Many of these models are quite powerful. However, they are often complex, species- or cell-type specific, and are largely concerned with modeling how crawling itself is produced.

Since we are interested in mapping the variability of cellular crawling with the goal of quantitatively comparing it with other forms of movement (e.g. swimming or gliding), we developed a more flexible and general tool for comparing the dynamics of crawling.

The approach

Our goal when embarking on this study was to generate a way to compare the movement of diverse types of crawling cells.

Generally, how to represent one's data and extract meaningful signals is a key, and often difficult, decision in computational studies. With organismal movement, this decision is often guided by the anatomy of the organism being studied. For example, in some organisms, the most important features might be the positions of the head, rear, and limbs over time. Anatomical features such as these lead to certain types of spatially stereotyped movement. For example, bilateral symmetry, dorsoventral patterning, and muscle contraction can lead to movements such as leg swings, head turns, or arm raises. This stereotypy has likely aided in the development of computational tools for mapping and comparing the behavior of animals.

However, the anatomical features that structure movement vary widely across organisms [14]. For example, the movement of many unicellular eukaryotes relies on morphological flexibility. These organisms lack clear signals of polarity *in situ* and rely on constant cellular deformation and remodeling to generate movement, a trait shared

with many motile cell types that constitute the tissues of multicellular organisms. Given the diversity of cellular shapes that can form during this type of movement, figuring out how best to capture these dynamics is not immediately obvious.

Here, we present a solution to this problem that relies on registering cells and computing key components of shape dynamics that are then used to generate a universal movement space via the TREBLE framework **[15]**. Briefly, TREBLE is a framework for building 'maps' of organismal movement and behavior (which we refer to here as 'movement spaces'). These maps contain information about how different movements relate to each other and help researchers identify common, continuous pathways between them. TREBLE is especially useful for comparative analyses involving many individuals or species since it can incorporate data from diverse sources in the construction of its maps.

Detailed methods

Data

All data analyzed here were published previously and are <u>publicly available</u>. Details on cell culturing and experimental conditions can be found in the original publication **[13]**.

Briefly, freely migrating *Dictyostelium discoideum* (n = 19 time series), cichlid fish (*Hypsophrys nicaraguensis*) keratocyte (n = 12), and human neutrophil-like HL60 cells (n = 22) were time-lapse-imaged on an upright microscope using cell-type specific media. All images were pre-processed in the same fashion. First, individual images were rotated to align the direction of movement with the y-axis. The rotated images were then rescaled so that the cell's area was equivalent to that of a circle with a 25 pixel diameter. Finally, the rotated and rescaled images were embedded into a 64x64 pixel frame. This pre-processing results in a set of cell images with standardized sizes and directions, facilitating comparative analyses across cell types with diverse shapes and sizes.

Analysis

All **code** generated and used for the pub is available in <ins>this GitHub repository</ins> (DOI: <ins>10.5281/zenodo.7195103</ins>), including all reference code and notebooks used for analysis.

The pre-processed images generated above were then used for all subsequent work in this pub. These analyses, and their associated methodologies, are laid out in detail in three fully interactive and editable notebooks available via <ins>GitHub</ins>.

Notebook 1: Data, shape components, and iterative window search

<ins>Notebook 1</ins> covers loading the pre-processed images and generating common 'shape components' using principal component analysis. It then goes on to cover how to run an iterative window search using the shape components. The goal of this search is to identify an 'optimal' window size to use for making a universal movement space (the theory and methodology of which are also covered in this notebook). Finally, we outline the creation of the movement space using the chosen window size.

Notebook 2: Exploring movement space

<ins>Notebook 2</ins> walks through the annotation of movement space, including calculation of geometric measures to describe cell shape, and comparing basic cell type differences in movement and geometry.

Notebook 3: Comparing cell type variance and temporal structure

<ins>Notebook 3</ins> builds on the first two to explore patterns of inter- and intra-specific variation among the cell types. First, movement variation is compared across cell types by assessing differences in occupation in, and trajectories through, movement space. It then covers how to measure temporal patterns in movement. Finally, we interrogate the relationship between cell shape and movement.

The results

A framework for mapping deformable movement

As outlined above ("The approach"), we processed video images of three cell types — *Dictyostelium* (slime mold), human HL60 cells, and cichlid fish keratocytes — to be the same size and orientation (Figure 1, Ai). Using principal component analysis (PCA), we identified 15 distinct shapes that represent the vast majority of possible cell shapes in the dataset (Figure 1, Aii and B). The first three components (25.79%, 11.78%, 8.53% variance explained, respectively; total = 46.10%) represented relatively simple shapes, namely horizontal (PC1), angled (PC2), and stretched (PC3) shapes (Figure 1, B). Subsequent components represented increasingly complex shapes that were determined by specific rules (see 'Shape component' panels in Figure 1, B). For example, PC4 represented cases in which a cell was bifurcated on the left (represented by the red, higher-likelihood blobs in the left-hand part of the 'Shape component' panel) and a single right-hand protrusion, with clear low-likelihood zones (in blue) separating these areas (Figure 1, B). A cell's shape at a given time point in the dataset could thus be thought of as some combination of these 15 shape types. A horizontally oriented, straight cell would score high for PC1 but not, say, PC4. This representation could then be used as the basis for figuring out how cell shapes compared to each other over time.

A reasonable next step after calculating these shape components would be to assess how every time point in the dataset relates to all others (e.g. with some form of clustering or classifying strategy). However, movements — be it of animals or individual cells — are temporally structured owing to factors such as inertia or biomechanical constraints [16]. Analyses of movement are therefore greatly benefitted by accounting for the timescales over which movements tend to occur. Given this, we employed the TREBLE framework [15] to analyze shape dynamics since it factors in this temporal variation. Specifically, we used TREBLE to identify an optimal window size (measured by number of video frames included) to sample the shape components (Figure 1, Aiii; for more details see "The approach" and the accompanying notebooks), generated highly-overlapping windows (separated by a step size of one frame), and created a movement space encompassing all cells in the dataset using the UMAP algorithm [17]

(Figure 1, Aiv). Given the density of temporal sampling employed by TREBLE, individual points in the resulting movement space are connected by continuous trajectories (Figure 1, Aiv), allowing robust analyses of the temporal evolution of cell morphodynamics.
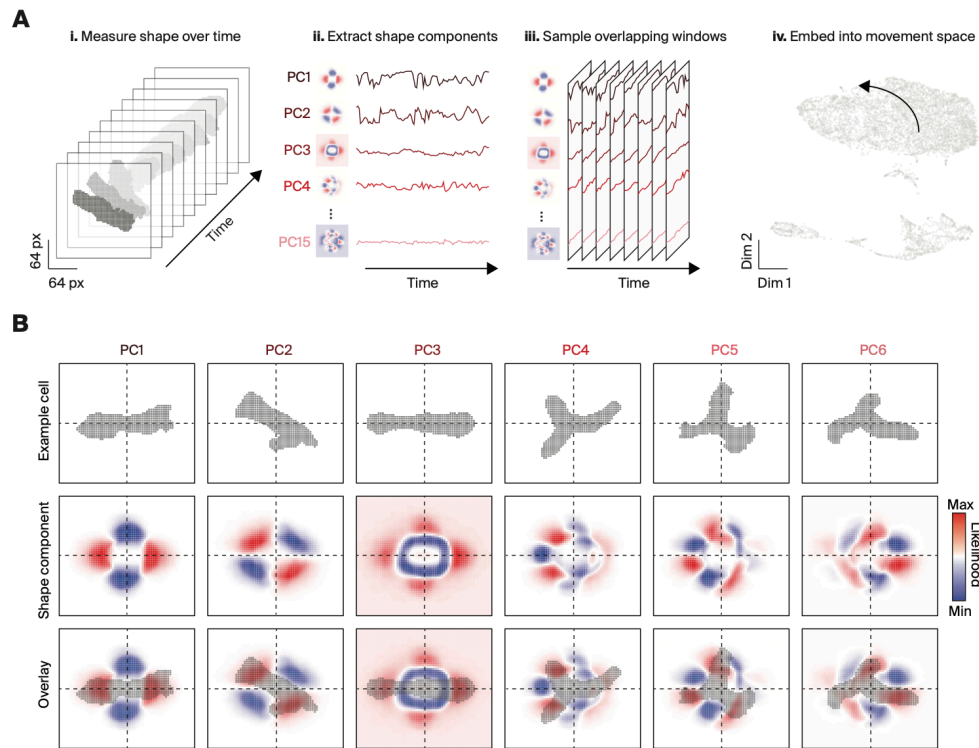
Figure 1

Overview of strategy for extracting 2D cell shapes from videos of crawling cells and mapping shapes across movement space over time.

(Ai) Cartoon demonstrating the representation of cell shape over time in the dataset. Cell images were segmented, oriented, and resized into 64 × 64 pixel matrices.

(Aii) Example shape components for a single cell and their values over time. Each component (PC1...15) is shown with its associated 2D eigenvector (blue = negative values; red = positive values).

(Aiii) Demonstration of the window-binning strategy used in the TREBLE framework. Shape components are extracted into overlapping temporal windows and are then embedded into a 2D movement space (Dim = dimension), Aiv.

(Aiv) The path through movement space in Aiv corresponds to the same timespan represented in Ai–Aiii.

(B) Expanded examples of shape components and their associated eigenvectors for the first six components (PC1–PC6). The first row contains representative cell shapes for each component. Below are the eigenvectors for each (labeled 'Shape component'). Increasingly red areas correspond to higher likelihoods of portions of the cell occurring in the region, increasingly blue correspond to lower likelihoods. The example cells and associated eigenvectors are overlaid in the bottom row, demonstrating the relationship between the two representations.

We next used the 2D "map" of behavior generated above to assess the overall distributions of movement patterns for the three cell types in the dataset: *Dictyostelium*, HL60, and keratoctyes (Figure 2, A). We found that each cell type was associated with a specific region of the map (Figure 2, B) and these regions were associated with specific cell shapes (Figure 2, C; Video 1). At first glance, it's clear that these shapes reflected differences in morphology possessed by the three cell types (Figure 2, A). However, they also differed in the amount of variation around the mean cell shape. For example, *Dictyostelium* cells appeared to possess greater diversity in cell shape (reflected by the "fuzziness" of the mean cell images) compared to keratoctyes (Figure 2, C). This suggests that, not only are these cell types identifiable by movement differences, but that each may possess unique qualities in the patterning and complexity of their movements.

Video 1

The relationship between physical and movement space coordinates.

Three representations of a single *Dictyostelium* trial are presented here. Leftmost is the raw image file of the trial ('Raw image'), middle is the oriented and segmented image ('Segmented cell'), and rightmost are the positions in movement space coordinates corresponding to the time points in the other two panels. Timepoint in the trial is indicated by color in the 'Segmented cell' and 'movement space position' panels (also represented by the counter on the bottom).

What aspects of shape and movement are associated with these differences? To address this we calculated several geometric measures describing cell shape: circularity (higher values = less circular), area, perimeter, major and minor axis, and displacement (the difference in the cell boundary between timepoints). We found that each measure had a characteristic distribution across movement space (Figure 2, D). For example, circularity varied between the left and right portions of movement space, mirrored by the measures of perimeter and major axis (which both also capture aspects of vertical extension) (Figure 2, D). On the other hand, displacement (which is a proxy for speed of movement) seemed to differ as a function of cell type. Keratocytes were associated with the lowest displacement values, HL60 were intermediate, and *Dictyostelium* were highest (Figure 2, D–E); and there was statistically significant

variation across cell types in this measurement, along with the other five geometric measures ([Figure 2](#), E). These results demonstrate the power of movement space analysis for separating cells along identifiable morphodynamics axes. Furthermore, it should be noted that these geometric measures are orthogonal to those used in the generation of the behavioral map, suggesting that the shape components captured relevant and identifiable aspects of cell morphodynamics.
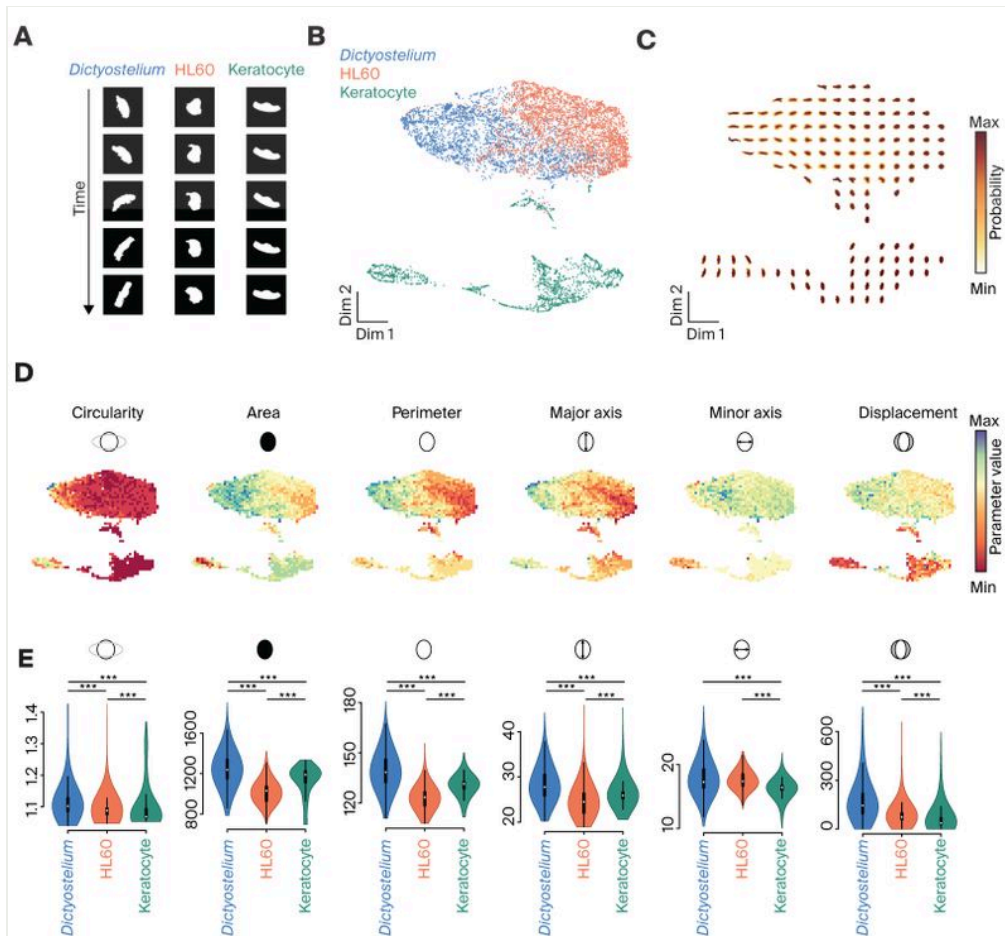
Figure 2

Characterizing cell type diversity in movement space.

(A) Example time series images of the three cell types in the dataset (*Dictyostelium*, HL60, and keratocytes).

(B) Movement space colored by cell type of origin (grey = *Dictyostelium*; blue = HL60; orange = keratocytes).

(C) Mean cell shapes as a function of movement space. We produced this image by binning points in movement space onto a 16 × 16 grid and then calculating the mean cell shape for all time points in each bin, plotted as heatmaps with probability represented by colors ranging from white (minimum) to dark red (maximum).

(D) The distribution across movement space for the six geometric measurements considered in this study.

(E) Violin plots comparing the six geometric measures as a function of cell type. Units in the y-axes correspond to the geometric measures labeled in the corresponding data in panel D. (*** = p < 0.001; Kruskal-Wallis test followed by Dunn's test).

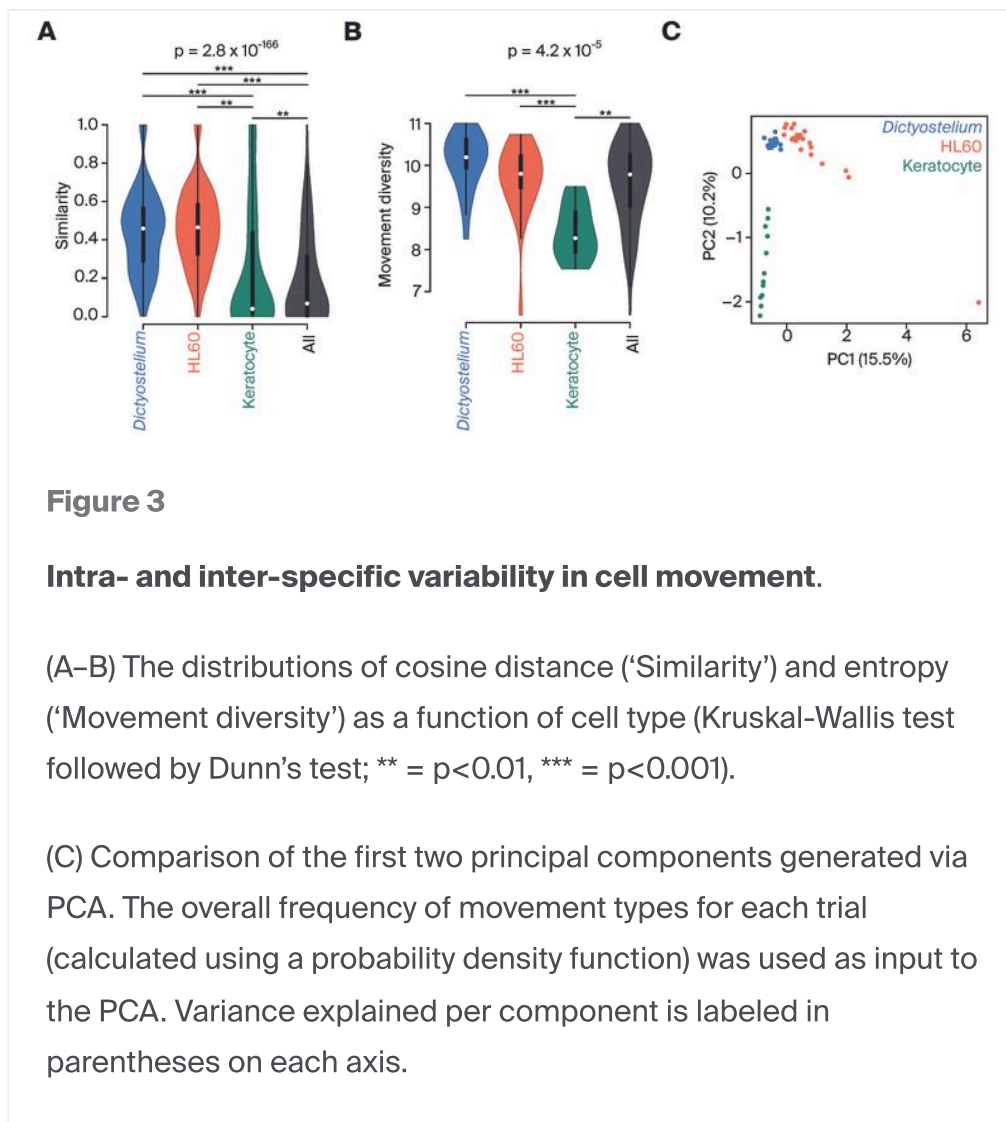## Cell movement varies across multiple axes

We next assessed the amount of movement diversity among the three cell types. Given the above analyses of mean cell shape and geometric parameters, it stood to reason that certain cell types (e.g. *Dictyostelium*) might show greater variation in morphodynamic patterns than others. To quantify this, we calculated two metrics: cosine distance ('**similarity**') and entropy ('**movement diversity**').

Briefly, **cosine distance**, or **similarity,** compares the behavior of any two cells. This is done by measuring the difference between where the cells went in movement space (and for how long). Essentially, this measure indicates how similarly individual cells of the same type tend to move. Comparing the similarity of all the cells in our dataset can thus let us glean if certain cell types share more or less movement identity with themselves, and how these patterns might relate to the overall similarity between cells in the dataset. Where cosine distance gives a sense of the similarity of overall movement patterns, entropy lets us infer *how* cell movement differs in complementary fashion.

Entropy, or **movement diversity**, is essentially a measure of the amount of movement space a single cell's movement patterns cover. Specifically, cells with more diverse movement patterns (i.e. positions more distributed throughout movement space) will be associated with higher entropy values.

We found that similarity varied broadly across cell types (Figure 3, A). *Dictyostelium* and HL60 cells displayed high degrees of intra-cell similarity while keratocytes were quite a bit more dissimilar to themselves, and significantly differed from the other two cell types (p = 0.001; Kruskal-Wallis test followed by Dunn's test; Figure 3, A). On the other hand, *Dictyostelium* (p < 0.0001; Dunn's test) and HL60 (p = 0.0003; Dunn's test) cells displayed significantly higher movement diversity compared to keratoctyes (Figure 3, B). These observations were mirrored by a principal components analysis of the movement patterns for all cells in the dataset (Figure 3, C). Comparing the first two

principal components, it's apparent that *Dictyostelium* cells produce a tight cluster with themselves, flanked by a similarly dense group of HL60 cells while the keratocyte cells were much more broadly distributed ([Figure 3](#), C), indicating that the three cell types can be separated by clear axes of movement variation. Taken together, we can conclude from these observations that there is a continuum in movement diversity between the three cell types and, interestingly, that the cell types with more diverse movement patterns (*Dictyostelium* and HL60) show more self-similarity. On the other hand, keratocytes display less diversity in movement but are also less self-similar, suggesting a potentially simpler movement program that can be expressed in a variety of ways. It's interesting to speculate on the biological correlates of this movement diversity. For example, might the broader distributions of keratocyte and HL60 movement profiles ([Figure 3](#), C) reflect the presence of multiple cellular states?

Figure 3

Intra- and inter-specific variability in cell movement.

(A–B) The distributions of cosine distance ('Similarity') and entropy ('Movement diversity') as a function of cell type (Kruskal-Wallis test followed by Dunn's test; ** = $p<0.01$, *** = $p<0.001$).

(C) Comparison of the first two principal components generated via PCA. The overall frequency of movement types for each trial (calculated using a probability density function) was used as input to the PCA. Variance explained per component is labeled in parentheses on each axis.

Temporal variation in movement is associated with unique structure-function relationships

Finally, we decided to explore whether the diversity of shape and movement dynamics observed above are associated with differences in how the three cell types sequence movement over time. A nice feature of representing movement in a continuous space is that one can extract statistical information about the order in which particular movements occur by analyzing changes in movement space position over time. A common way to infer high-level patterns in the sequencing of movement is to measure the autocorrelation (i.e. correlation to self) of position in movement space over time (see [15] and [18]). Intuitively, the movements of organisms with more stereotyped or less dynamic behavior will often be more correlated over longer periods of time. On the other hand, organisms that switch between movement types frequently and express more varied sequences of movements may display less correlated temporal patterns.

Measuring the movement autocorrelation of the three cell types demonstrated that keratocytes had much longer decays than the other cells (Figure 4, A), suggesting that these cells possess more stereotyped movement patterns (and corroborating the entropy analyses in Figure 3, B). In addition to autocorrelation, we also examined the distribution of persistence in different portions of movement space for each cell type. Here, cells with more dynamic movement will tend to distribute their movement timing broadly, while more stereotyped movement patterns may display greater persistence in specific regions of movement space. As with the autocorrelation analyses, keratocytes differed from the other two cell types, displaying significantly longer periods of persistence than both HL60 (p<0.001; Dunn's test) and *Dictyostelium* (p<0.001; Dunn's test) (Figure 4, B–C).
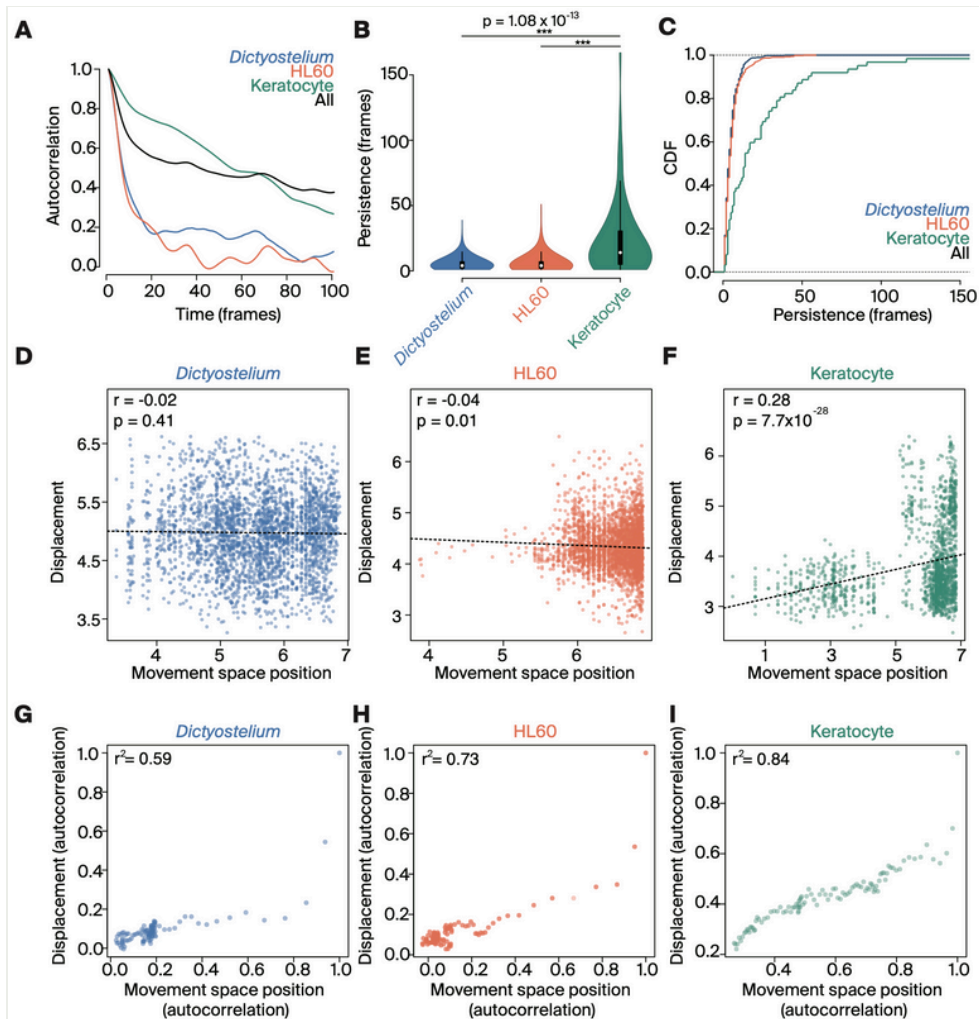
Figure 4

Temporal variation and structure-function relationships.

(A) The autocorrelation distributions of movement space position for *Dictyostelium*, HL60, and keratocytes.

(B) The distributions of persistence times across movement space (Kruskal-Wallis test followed by Dunn's test; *** = p < 0.001).

(C) Cumulative density functions of persistence time, highlighting the presence of much longer persistence in certain regions of movement space among keratocytes.

(D–F) Scatterplots of the relationship between movement space position (as a marker of cell shape dynamics, or 'structure') and displacement ('function') for *Dictyostelium* (D), HL60 (E), and keratocytes (F). Statistics are from Pearson's correlation tests.

A notable feature of cellular crawling is that a variety of cell morphologies can produce similar movement outcomes, representing a form of 'many-to-one' mapping between cell shape and movement. Given the above observations, we wondered whether or not the variation in temporal structure between the three cells might be related to differences in structure-function mappings during movement. To test this, we compared the distributions of displacement (representing movement output; 'function') and movement space position (i.e. complex morphological state; 'structure') and found strong differences in the relationships between these two measures across the cell types. Among *Dictyostelium* cells, there was no discernible relationship between movement space position and displacement (r = −0.02, p = 0.41; Pearson's correlation; Figure 4, D), strongly indicating the presence of many-to-one structure-function mapping. HL60 cells also showed little correlation, though the correlation was significant, suggesting a stronger relationship between cellular morphology and movement type than *Dictyostelium* (r = −0.04, p = 0.01; Figure 4, E). On the other hand, there was a significant correlation present among keratocytes (r = 0.28, p = 7.7x10^{28}; Figure 4, F), suggesting a comparatively strict relationship between cell shape and movement. Taken together, these results demonstrate a continuum of structure-function relationships exist among the cells tested. On one end, *Dictyostelium* possesses many degrees of freedom in its movement generation while keratocytes are comparatively quite restricted.

This continuum was even more present when factoring in temporal variation (in the form of the autocorrelation of movement space position and displacement). One can conceptualize this relationship as representing the dynamic relationship between cell shape and movement. Cases in which the two are tightly related indicate a narrow bandwidth of possible cell shape dynamics that are able to produce movement. On the other hand, cases in which the two distributions are less related reflect scenarios in which cell shape is able to vary more independently of movement. Here, as above, we found a continuum of these types of relationships. *Dictyostelium* possessed relatively less of a connection between temporal variation in structure-function (r^2 = 0.59; Figure 4, G), HL60 was in the middle (r^2 = 0.73; Figure 4, H), and keratocytes displayed a strong relationship between the two (r^2 = 0.84; Figure 4, I). These results suggest that variation in the temporal structure of movement is coupled with distinct structure-function relationships. Furthermore, this finding is notable in that it ties

analyses of cellular motility with discrete structural properties that have well-described biological mechanisms (e.g. cytoskeletal remodeling and adhesion genes), providing a potential framework for the high-throughput association of molecular dynamics with complex morphological and movement phenotypes.

Key takeaways

Our computational framework solves a number of key problems in handling and analyzing large cellular motility datasets.

We can represent complex changes in cell shape using an interpretable, low-dimensional space which we can readily use to dissect variation across individuals, cell types, and species. In addition, we found that we are able to link the dynamics of cell shape and the production of movement using a simple measure, opening up many possibilities for comparative analyses of cellular crawling across evolutionary scales.

Our framework is just one of many options for studying and modeling cellular movement. In particular, we did not build any predictive or generative components into this work. We therefore consider this framework as a tool to complement, rather than replace, the host of models that exist for this purpose. That said, we do believe it provides a very useful and unique tool for approaching large-scale comparative studies of cellular motility.

By leveraging the framework, we were able to uncover a variety of sub-modalities of cellular crawling. We found that crawling was associated with spatiotemporal variation across multiple aspects of cell shape and geometry. Cells displayed distinct morphodynamic profiles that segregated both cell type and movement state. Notably, these differences included unique relationships between dynamic changes in cell shape and kinematic output (i.e. speed). This finding suggests that, within a given cell type, multiple shapes can achieve similar movement outcomes. These patterns may indicate the presence of multiple movement types that could be linked to cellular state or some other variable, further refining the categorization of this complex behavior in space and time.

Next steps

We are now phenotyping a large cohort of organisms with a variety of motility types with the goal of continuing to expand the movement space presented here. We are excited to explore which axes of morphodynamics and movement will be most variable across these organisms. In addition, we are especially interested in identifying conserved and novel motility regimes across evolution (and the biological mechanisms that regulate them). Expanding this framework to include other movement types, such as ciliary swimming, will be a first step.

References

1   Miller MB, Bassler BL. (2001). Quorum Sensing in Bacteria.
    https://doi.org/10.1146/annurev.micro.55.1.165

2   Swafford AJM, Oakley TH. (2017). Multimodal sensorimotor system in unicellular zoospores of a fungus. https://doi.org/10.1242/jeb.163196

3   Coyle SM, Flaum EM, Li H, Krishnamurthy D, Prakash M. (2019). Coupled Active Systems Encode an Emergent Hunting Behavior in the Unicellular Predator Lacrymaria olor. https://doi.org/10.1016/j.cub.2019.09.034

4   Miller CT, Gire D, Hoke K, Huk AC, Kelley D, Leopold DA, Smear MC, Theunissen F, Yartsev M, Niell CM. (2022). Natural behavior is the language of the brain.
    https://doi.org/10.1016/j.cub.2022.03.031

5   Othmer HG. (2018). Eukaryotic cell dynamics from crawlers to swimmers.
    https://doi.org/10.1002/wcms.1376

6   Neilson MP, Veltman DM, van Haastert PJM, Webb SD, Mackenzie JA, Insall RH. (2011). Chemotaxis: A Feedback-Based Computational Model Robustly Predicts Multiple Aspects of Real Cell Behaviour.
    https://doi.org/10.1371/journal.pbio.1000618

7   Shi C, Huang C-H, Devreotes PN, Iglesias PA. (2013). Interaction of Motility, Directional Sensing, and Polarity Modules Recreates the Behaviors of

Chemotaxing Cells. https://doi.org/10.1371/journal.pcbi.1003122

8   Miao Y, Bhattacharya S, Edwards M, Cai H, Inoue T, Iglesias PA, Devreotes PN. (2017). Altering the threshold of an excitable signal transduction network changes cell migratory modes. https://doi.org/10.1038/ncb3495

9   Cao Y, Ghabache E, Rappel W-J. (2019). Plasticity of cell migration resulting from mechanochemical coupling. https://doi.org/10.7554/elife.48478

10 Bhattacharya S, Banerjee T, Miao Y, Zhan H, Devreotes PN, Iglesias PA. (2020). Traveling and standing waves mediate pattern formation in cellular protrusions. https://doi.org/10.1126/sciadv.aay7682

11 Edelstein-Keshet L, Holmes WR, Zajac M, Dutot M. (2013). From simple to detailed models for cell polarization. https://doi.org/10.1098/rstb.2013.0003

12 Alonso S, Stange M, Beta C. (2018). Modeling random crawling, membrane deformation and intracellular polarity of motile amoeboid cells. https://doi.org/10.1371/journal.pone.0201977

13 Imoto D, Saito N, Nakajima A, Honda G, Ishida M, Sugita T, Ishihara S, Katagiri K, Okimura C, Iwadate Y, Sawai S. (2021). Comparative mapping of crawling-cell morphodynamics in deep learning-based feature space. https://doi.org/10.1371/journal.pcbi.1009237

14 Miyata M, Robinson RC, Uyeda TQP, Fukumori Y, Fukushima S, Haruta S, Homma M, Inaba K, Ito M, Kaito C, Kato K, Kenri T, Kinosita Y, Kojima S, Minamino T, Mori H, Nakamura S, Nakane D, Nakayama K, Nishiyama M, Shibata S, Shimabukuro K, Tamakoshi M, Taoka A, Tashiro Y, Tulum I, Wada H, Wakabayashi K. (2020). Tree of motility – A proposed history of motility systems in the tree of life. https://doi.org/10.1111/gtc.12737

15 York RA, Carreira-Rosario A, Giocomo LM, Clandinin TR. (2020). Flexible analysis of animal behavior via time-resolved manifold embedding. https://doi.org/10.1101/2020.09.30.321406

16 Katsov AY, Freifeld L, Horowitz M, Kuehn S, Clandinin TR. (2017). Dynamic structure of locomotor behavior in walking fruit flies. https://doi.org/10.7554/elife.26410

17 McInnes L, Healy J, Melville J. (2018). UMAP: Uniform Manifold Approximation and Projection for Dimension Reduction. https://doi.org/10.48550/ARXIV.1802.03426

18 York RA, Brezovec LE, Coughlan J, Herbst S, Krieger A, Lee S-Y, Pratt B, Smart AD, Song E, Suvorov A, Matute DR, Tuthill JC, Clandinin TR. (2022). The

evolutionary trajectory of drosophilid walking.
https://doi.org/10.1016/j.cub.2022.05.039